ADVANCES IN ATMOSPHERIC SCIENCES, VOL. 20, NO. 4, 2003, PP. 511–529

Seasonal Characteristics of Precipitation in 1998 over East Asia as Derived from TRMM PR

FU Yunfei*[1,2] (傅云飞), LIN Yihua[2] (林一骅), Guosheng LIU**[3] (刘国胜), and WANG Qiang[4] (王 强)

[1] *Department of Earth and Space Sciences, University of Science and Technology of China, Hefei* 230026

[2] *LASG, Institute of Atmospheric Physics, Chinese Academy of Sciences, Beijing* 100029

[3] *Department of Meteorology, Florida State University, USA*

[4] *School for Continuing Education, University of Science and Technology of China, Hefei* 230026

(Received April 10, 2002; revised April 10, 2003)

ABSTRACT

Precipitation radar data derived from the Tropical Rainfall Measuring Mission (TRMM) satellite are used to study precipitation characteristics in 1998 over East Asia (10°–38°N, 100°–145°E), especially over mid-latitude land (continental land) and ocean (East China Sea and South China Sea). Results are compared with precipitations in the tropics. Yearly statistics show dominant stratiform rain events over East Asia (about 83.7% by area fraction) contributing to 50% of the total precipitation. Deep convective rains contribute 48% to the total precipitation with a 13.7% area fraction. The statistics also show the unimportance of warm convective rain in East Asia, contributing 1.5% to the total precipitation with a 2.7% area fraction. On a seasonal scale, the results indicate that the rainfall ratio of stratiform rain to deep convective rain is proportional to their rainfall pixel ratio. Seasonal precipitation patterns compare well between Global Precipitation Climatology Project rainfall and TRMM PR measurements except in summer. Studies indicate a clear opposite shift of rainfall amount and events between deep convective and stratiform rains in the meridional in East Asia, which corresponds to the alternative activities of summer monsoon and winter monsoon in the region. The vertical structures of precipitation also exhibit strong seasonal variability in precipitation Contoured Rainrate by Altitude Diagrams (CRADs) and mean profiles in the mid-latitudes of East Asia. However, these structures in the South China Sea are of a tropical type except in winter. The analysis of CRADs reveals a wide range of surface rainfall rates for most deep convective rains, especially in the continental land, and light rain rate for most stratiform rains in East Asia, regardless of over land or ocean.

Key words: TRMM PR, seasonal variability, precipitation structure

1. Introduction

In the Asian monsoon system, the structure of the circulation system in East Asia is different from that in the Indian sub-continent. These are respectively called the East Asian monsoon system and the Indian monsoon system (Krishnamuti and Bhalme, 1976; Tao and Chen, 1987; Chen et al., 1992). Both systems also have different rules of interaction between the coupled ocean/atmosphere systems (Lau and Li, 1984; Lau et al., 1988; Yasunari, 1990, 1991; Fu and Huang, 1997). Associated with the activities of the monsoon, the distributions of precipitation and heavy rainfall events, especially during summer, have been studied by many authors (Ding and Reiter, 1982; Matsumoto, 1985; Lau et al., 1988; Ninomiya, 1984, 2000; Ninomiya and Murakami, 1987). Inside the East Asia monsoon, a special weather system over East Asia known as the "Meiyu" front (or "Baiu" front in Japan) and its precipitation, has been given importance from scientists, and many experiments, such as TAMEX (Taiwan Area Mesosclae Experiment) (Kuo and Chen, 1990) and the recent GAME/HUBEX (Huaihe Basin Experiment) (Ding et al., 2001), have been made in the region. Although features of clouds in East Asia have been analyzed by IR (Infrared Radiation) data of GMS (Geostationary Meteorological Satellites) (Murakami, 1983;

*E-mail: fyf@ustc.edu.dn, **E-mail: liug@met.fsu.edu

Takeda and Iwaski, 1987), our knowledge of characteristics of precipitation in East Asia, such as distributions of precipitation types (convective or stratiform rainfalls) and vertical structures of precipitation (precipitation profiles), is still limited by our ground based and space based observations.

A better knowledge of precipitation types and their vertical structures is important both for understanding cloud dynamics and microphysical processes including latent heating release (Fujiyoshi et al., 1980; Houze, 1981; Szoke et al., 1986; Hobbs, 1989; Liu and Takeda, 1989; Zipser and Lutz, 1994), and for improving satellite precipitation algorithms (e.g., Wilheit et al., 1977; Petty, 1994; Kummerow and Giglio, 1994). Physical retrieval of precipitation on the surface from satellite microwave measurements requires the knowledge of vertical distributions of hydrometeors because microwave brightness temperatures are very sensitive to these profiles (Smith and Mugnai, 1988; Adler et al., 1991; Fulton and Heymsfield, 1991; Fu and Liu, 2001). The knowledge is also helpful in developing parameterization of rain processes in numerical models.

In previous studies (Liu and Fu, 2001; Fu and Liu, 2001), the authors investigated characteristics of precipitation profiles over the tropics using TRMM (Tropical Rainfall Measuring Mission) PR (Precipitation Radar) observation data. As a continued work, we have two objectives in this study. The first is to investigate horizontal distributions of precipitation events in East Asia on a seasonal scale, and the other is to generalize precipitation profile patterns in the region.

2. Data

The data, 2A25, used in this study are a standard TRMM product derived from TRMM PR. According to the properties of the PR, the data of 2A25 supply rainfall intensity with a horizontal resolution of 4.3 km at the nadir and a vertical resolution of 250 m from the Earth's surface to 20 km altitude. Furthermore, the data also contain information on rainfall types based on the vertical pattern of the profiles (we used the classification based on the TRMM V method; Awaka et al., 1998). A rain profile is classified as stratiform if PR detects a bright band near the freezing level. If no bright band exists and any value of radar reflectivity in the beam exceeds a predetermined value of about 39 dBZ, the profile is classified as connective. Profiles are labeled as "others" when they do not meet the definitions of either stratiform or convective rain. Among convective rains, we can group warm rains (or shallow convective) and deep convective rains. The warm rain's echo top is below the freezing level. The deep convective rains are convective rains with the echo top above the freezing level.

The data of 2A25 in each swath cover a region between 38°S and 38°N, and there are nearly 16 swaths everyday. For convenience, a sub-dataset of precipitation profiles is generated in the East Asia region (10°–38°N, 100°–145°E) from the 2A25. In the dataset, we pick all precipitation profiles at each scan along swaths from 1 January to 31 December 1998. We also define the precipitating case (or pixels) as having a nonzero rain rate at 500 m above the surface in each profile to keep the retrieved rain rate of the low atmosphere uncontaminated. The total number of pixels in our sample dataset is 129,432,120, and of them 70,822,301, or about 5.5%, are precipitating.

To reveal details in East Asian precipitation, three regions are selected. They are the mid-eastern mainland of China (25°–35°N, 110°–120°E, called continental land for short, which covers the Huaihe River basin and Yangtze River valley), the East China Sea (25°–35°N, 122°–130°E), and the South China Sea (10°–20°N, 110°–120°E). The three regions in East Asia are regarded as key representatives where rainfalls are affected greatly by the East Asian monsoon. During summer, precipitation intensities over the continental land and the East China Sea are always associated with states of Meiyu, while during winter, activities of cold fronts also induce variations of precipitation in both regions. Close attention is also paid to the region of the South China Sea, considering strong activities of deep convective rains over there. Knowledge of characteristics of precipitation is limited in this region because of poor observations. Precipitation characteristics over the continental land and the East China Sea represent rainfall information in the mid-latitudes of East Asia. On the other hand, precipitations in the South China Sea are possibly of tropical features. It is helpful to understand features between the land and ocean, and between the mid-latitudes and the tropics, when comparing precipitations in the three regions.

3. Results

3.1 *Sample statistics*

Two variables, area fraction and rain fraction, are defined to discuss the precipitation statistics. The area fraction is the number ratio of rain pixels of a specific rain type (stratiform or convective) to the raining pixels, which represents the occurrence frequency of a specific rain type. Similarly, the rain fraction is the ratio of rain amount generated by a specific rain type to total rain amount, which represents the contribution of a specific rain type to the total rain amount.

Table 1. Statistics of sample radar precipitation

Rain Type	Number of Precipitation pixels	Area Fraction	Rain Total Fraction	Average Rainfall Rate
Stratiform	5,579,720	78.8%(83.7%)*	50.1%	1.7 mm h^{-1}
Deep Convection	903,676	12.8%(13.6%)*	47.5%	10.2 mm h^{-1}
Warm Convection	180,669	2.6%(2.7%)*	1.5%	1.6 mm h^{-1}
Other	418,236	5.8%	0.9%	0.4 mm h^{-1}

* Percentages in the parenthesis indicate the fractions without counting "other" as precipitating profiles.

The characteristics of the precipitating samples used in the analysis are shown in Table 1. Of the precipitating profiles, only 5.8% are classified as "other", which is very different from what happens in the tropical ocean (about 44.8%; Liu and Fu, 2001), perhaps due to the use of version 4 TRMM data in our previous work. Such type of rainfall is too light to meet the threshold for convective rain, and its contribution to total rainfall is very small (only ∼0.9%) because this type is all light rains. If we do not count these profiles, the area fractions for stratiform, deep convective, and warm convective rain are 83.7%, 13.6%, and 2.7%, respectively. Warm convective rain contributes to about 1.5% of the total precipitation. It is obvious that warm rainfalls are not important rain events in East Asia. We do not discuss warm convective rains in this study.

Table 1 also clearly shows that the contribution to the total precipitation by deep convective rain (47.5%) is comparable to that by stratiform rain (50.1%) although the former only has 13.6% in area fraction, whereas the latter has 83.7%. In the tropics, the contributions by stratiform rain (79.9% area fraction) and deep convective rain (11.5% area fraction) are almost equally important, i.e., about 45% by stratiform and 42% by deep convective rain (Liu and Fu, 2001). As for averaged rainfall rate of stratiform and deep convective in East Asia, these values are 1.7 mm h^{-1} and 10.2 mm h^{-1}, respectively, which are greater than those in the tropics (1.3 mm h^{-1} for stratiform and 8.6 mm h^{-1} for deep convective). This feature exposes the stronger precipitation intensity in East Asia than in the tropics.

3.2 *Horizontal distribution of rain events*

Precipitation characteristics of seasonal variations in East Asia can be found in the horizontal distribution of precipitation as shown in Fig. 1. The left panel of the figure is generated from the Global Precipitation Climatology Project (GPCP) archived by NASA (Huffman et al., 1995), and the right panel is averaged rainfall rate from 2A25 data that is calculated for each $2.5^\circ \times 2.5^\circ$ box in four seasons. Precipitations in GPCP are a merged product (with 2.5° horizontal resolution) of raingauge measurements, satellite retrievals and numerical model outputs. Here, we define conventionally December, January, and February as the winter season, March, April, and May as spring, June, July, and August as summer, and September, October, and November as autumn. Generally, the rainfall patterns from the two outputs are very close in winter, spring, and autumn. However, in summer there exists a relative difference in rainfall pattern and amplitude between the two datasets. It seems that the magnitude of surface rainfall estimated by GPCP is larger than that by TRMM PR detections. It is hard to say which one generates more accurate precipitation. We are not going to say too much on that complex problem here. Figure 1 gives us the reliability of TRMM PR observations in East Asia as well as in the tropics.

The area fraction distributions of deep convective and stratiform rains in the four seasons are shown in Fig. 2. It reveals that stratiform precipitations in East Asia are the dominant form of precipitation in each season. Basically, the area fraction of stratiform rains can reach to more than 90% in East Asia. For deep convective rains, its area fraction does not exceed 30%. The figure indicates large values of stratiform rain area fraction in the northern part of East Asia, in contrast to the high frequency of deep convective rains in the southern part. It is clear there is a northward shift of deep convective rains in the area fraction map of East Asia from winter to spring, and a southward movement from summer to autumn. Such movement is opposite to the stratiform rain movement. This illustrates the seasonal variation of precipitation in East Asia, i.e. deep convective rain accompanying the summer monsoon northward extension at the end of the winter season, while at the end of summer and activities of the cold front, deep convective rains withdraw from the continent of East Asia, and startiform rains are dominant in the region. This means the activity of deep convection may be regarded as a good index for the summer the monsoon, and that of stratiform rains for the winter monsoon, in the mid-latitudes of East Asia.

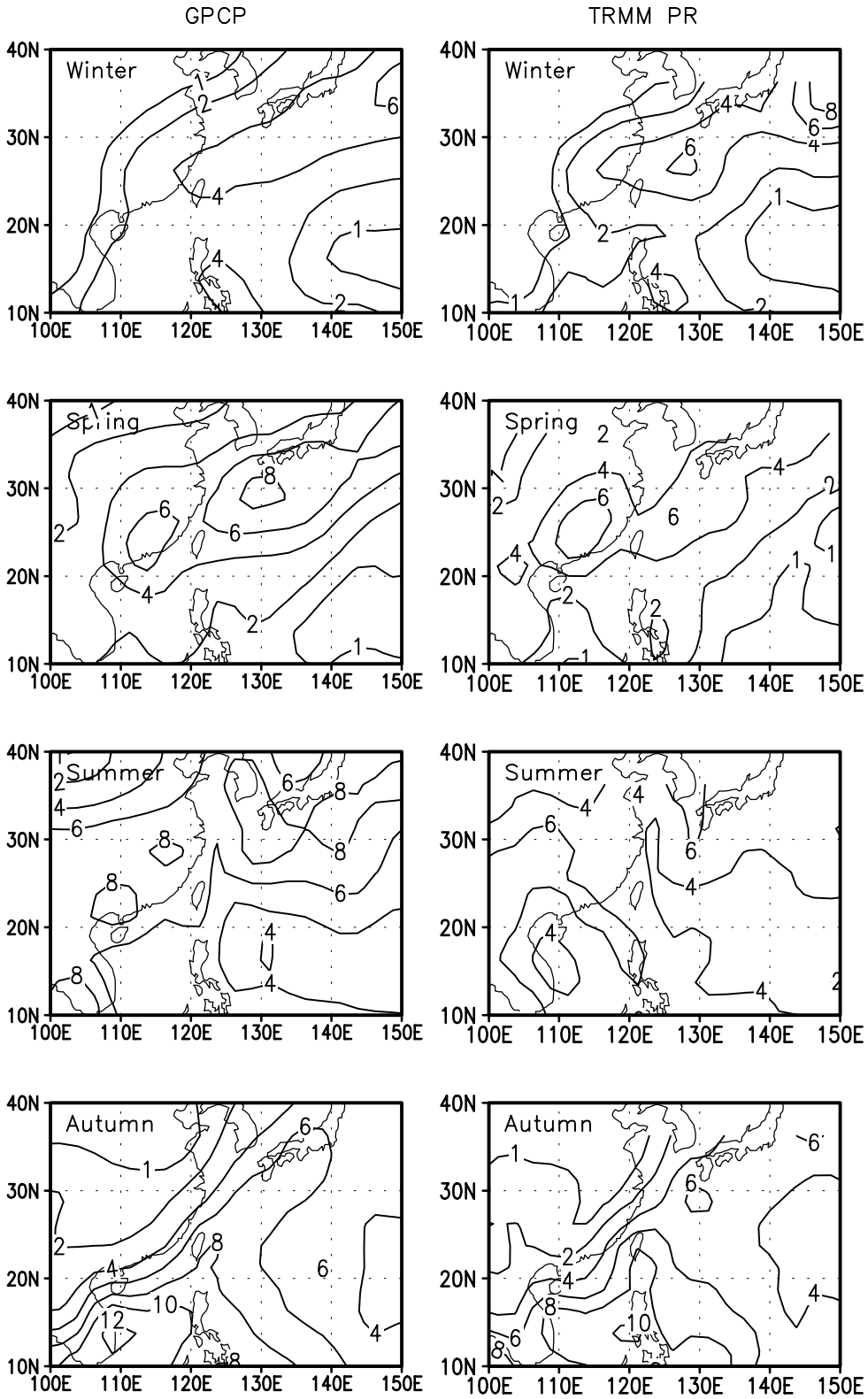

Fig. 1. Distributions of seasonal mean rainfall rate (mm d^{-1}) in 1998 produced by using GPCP (left panel) data and TRMM PR (right panel).

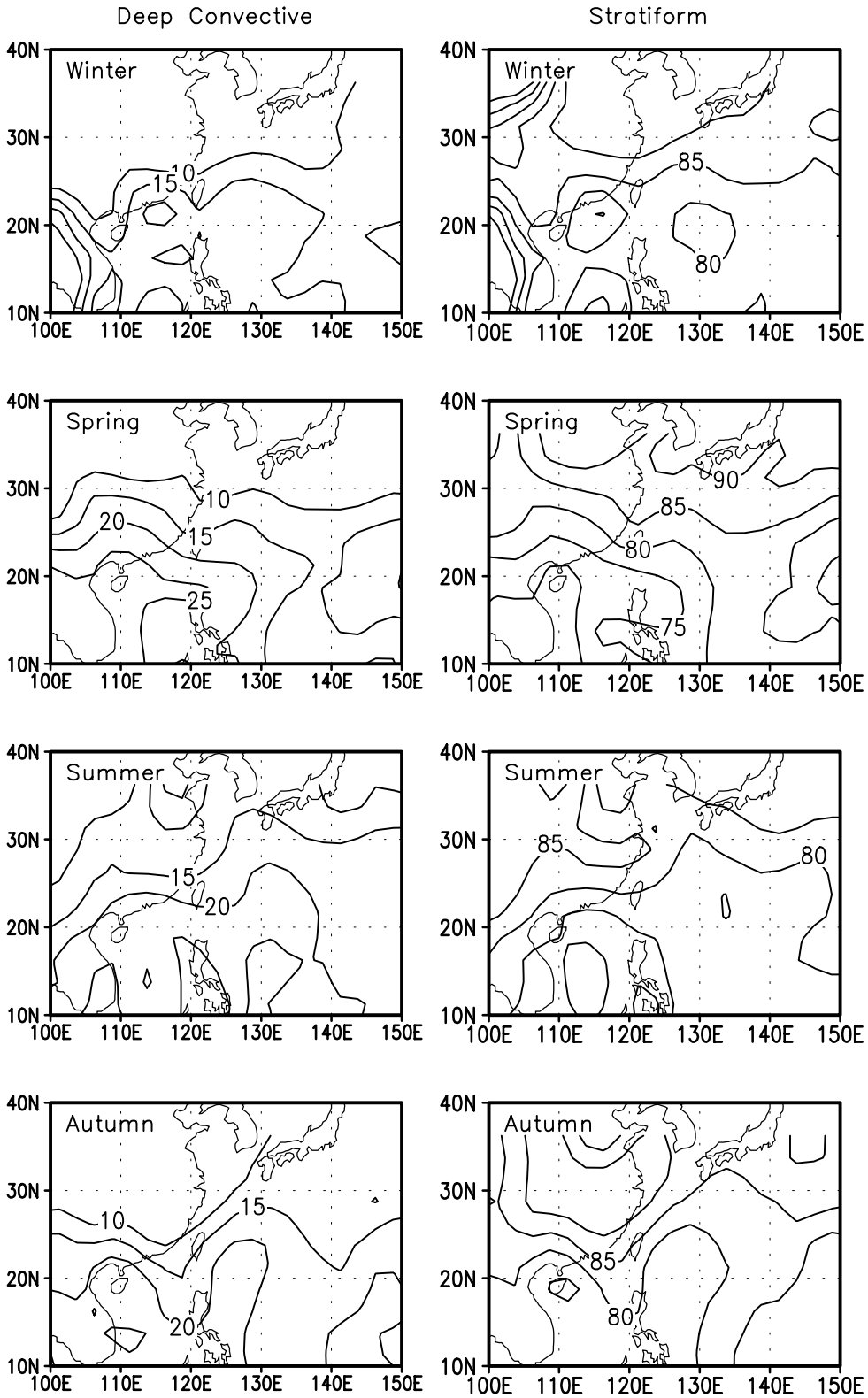

Fig. 2. Horizontal distributions of the area fraction for deep convective (left panel) and stratiform (right panel) to total rain numbers.

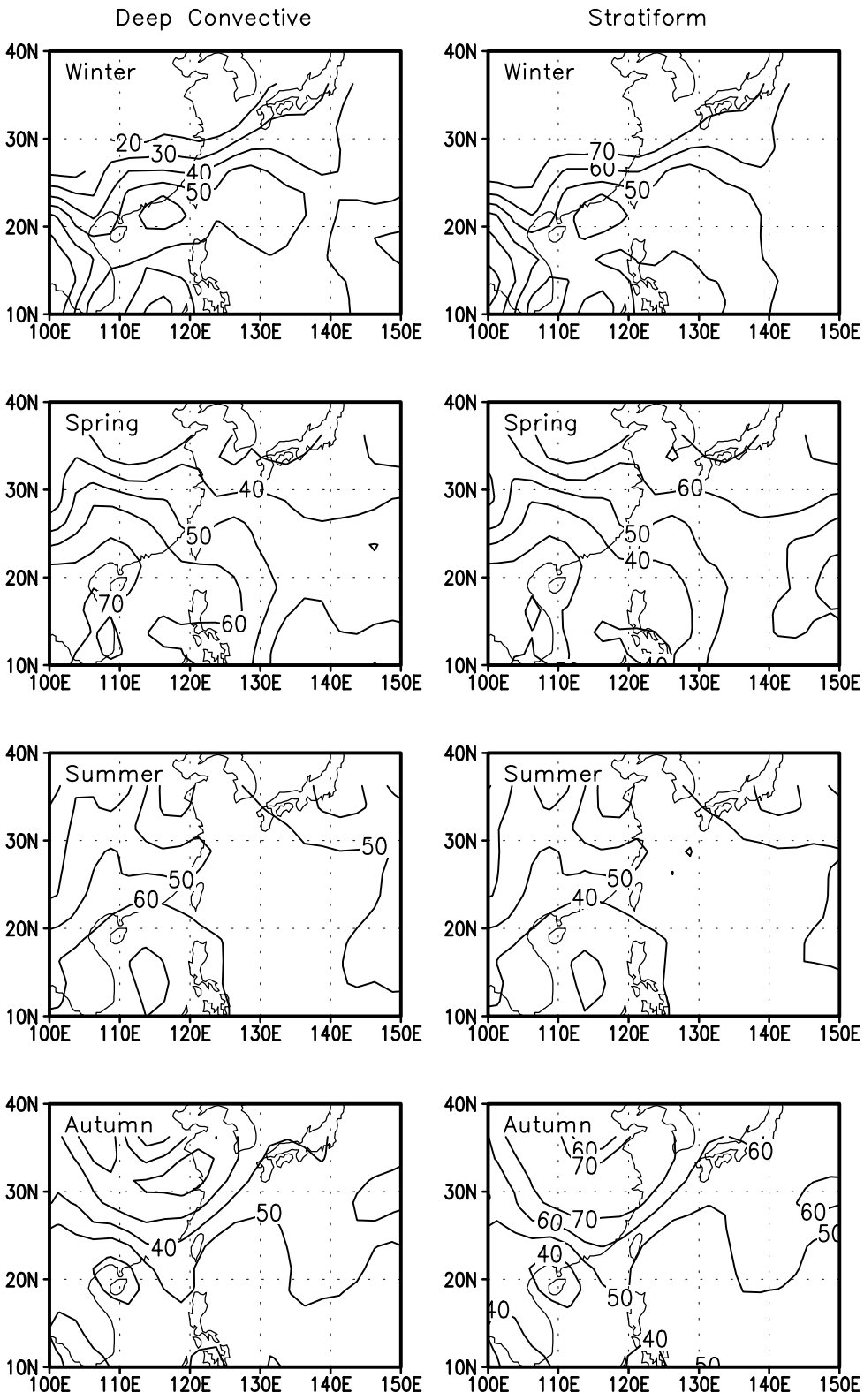

Fig. 3. Horizontal distributions of the rain fraction for deep convection (left panel) and stratiform (right panel) to rainfall total.

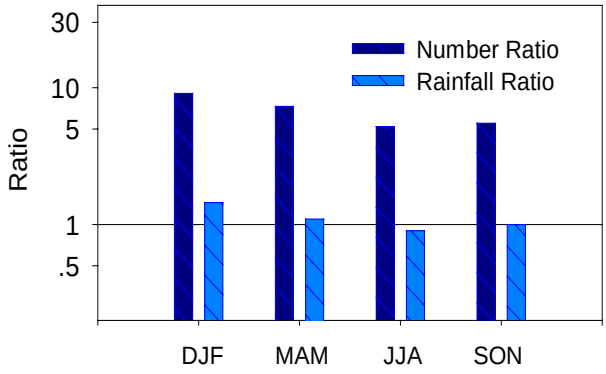

Fig. 4. Number ratio of stratiform pixels to deep convective pixels, and rainfall ratio of both rain types in four seasons.

As mentioned in section 3.1, deep convective rain contributes almost an equal amount to total rain as stratiform rain although the former's area fraction is only one-sixth of the latter's. The distribution of rain fraction can be found in Fig. 3. It shows that seasonal variations of these precipitations in East Asia are also clear on alternating domains of rainfall amount in space. Basically, stratiform and deep convective rains contribute majority rainfall (more than 50%) to total rain in northern and southern East Asia respectively. This feature is more remarkable in autumn and winter. However, both stratiform and deep convective rains produce almost equal amounts of rainfall to total rainfall in the middle part of East Asia, especially in middle-eastern China, and this feature is more clear in spring and summer.

The relationship between area fraction and rain fraction in East Asia is plotted in Fig. 4. We define in the figure the number ratio as the ratio of stratiform's area fraction to that of the deep convective rain, and the rainfall ratio as the ratio of stratiform's rain fraction to that of the deep convective rain. Although there is variation of the number ratio and rainfall ratio with the seasons, the ratio of the number ratio to the rainfall ratio is almost a constant, about 6, in each season. That means that the ratio of surface rainfalls produced by stratiform and deep convective rains is proportional to numbers of both rain types. Such a feature can be seen in the three regions, continental land, the East China Sea, and the South China Sea.

3.3 *Vertical structures of precipitation*

Yuter and Houze (1995) successfully used a statistical method, the Contoured Frequency by Altitude Diagrams (CFADs), to display the statistical distributions of the storm properties. However, the CFAD method has a side effect of increasing the percentages at the top of the storm where there are fewer data points. In order to overcome such weakness, we designed another statistical method, the Contoured Rainrate by Altitude Diagrams (CRADs), to reveal the averaged vertical structure of precipitation. The CRAD is constructed with height on the y-axis and rainfall rate on the x-axis. Contours describing rainrates normalized by total numbers of precipitation profiles for a given rain type are then plotted in this domain. We found that the differences in vertical distributions between convective and stratiform are very clear at the CRADs.

Figures 5a and 5b plot CRADs for deep convective and stratiform rains, respectively, in the continental land, the East China Sea, and the South China Sea at each season of 1998. Obviously different patterns between deep convective and stratiform rain can be found by comparing both figures, which shows different distributions of hydrometeors in the vertical for both rain types. For each rain type, the seasonal variation is clearly shown in distributions of CRADs in mid-latitude East Asia, continental land, and ocean, due to the seasonal variation of the freezing level. In the South China Sea, the CRAD patterns for each rain type are nearly the same except in winter. So, the seasonal variability in the South China Sea can be neglected from spring to autumn, which is also clear in Fig. 7. For stratiform rains, they have a narrow CRAD below the freezing level if comparing with convective rains. The contour of 0.25 mm h^{-1} covers the range only from 0.5 mm h^{-1} to 3.5 mm h^{-1} at 2 km. The maximum CRAD occurs between 1 mm h^{-1} and 2 mm h^{-1} at 2 km. The CRADs of deep convective distribute very wide below the freezing level. The 0.25 mm h^{-1}contour ranges from 2 mm h^{-1} to more than 20 mm h^{-1} at 2 km. These differences between the two rain types express a wide range of surface rainfall rate for most deep convective rains, and a light rain rate for most stratiform rains in East Asia, regardless of being over land or ocean. These differences also reveal distinctive latent heating structures between convective and stratiform, i.e. a bell-shape heating profile of convective rains with maximum heating in the mid troposphere while a dipole heating profile of stratiform rains with heating in the mid and cooling in the lower troposphere (Tao et al. 1993). Differences among deep convective rains also display their wider range of surface rain rate over the continental land than over the oceanic region (Fig. 5a). For stratiform rains, their surface rainfall rates are wider in the South China Sea than in the mid-latitude region (Fig. 5b).

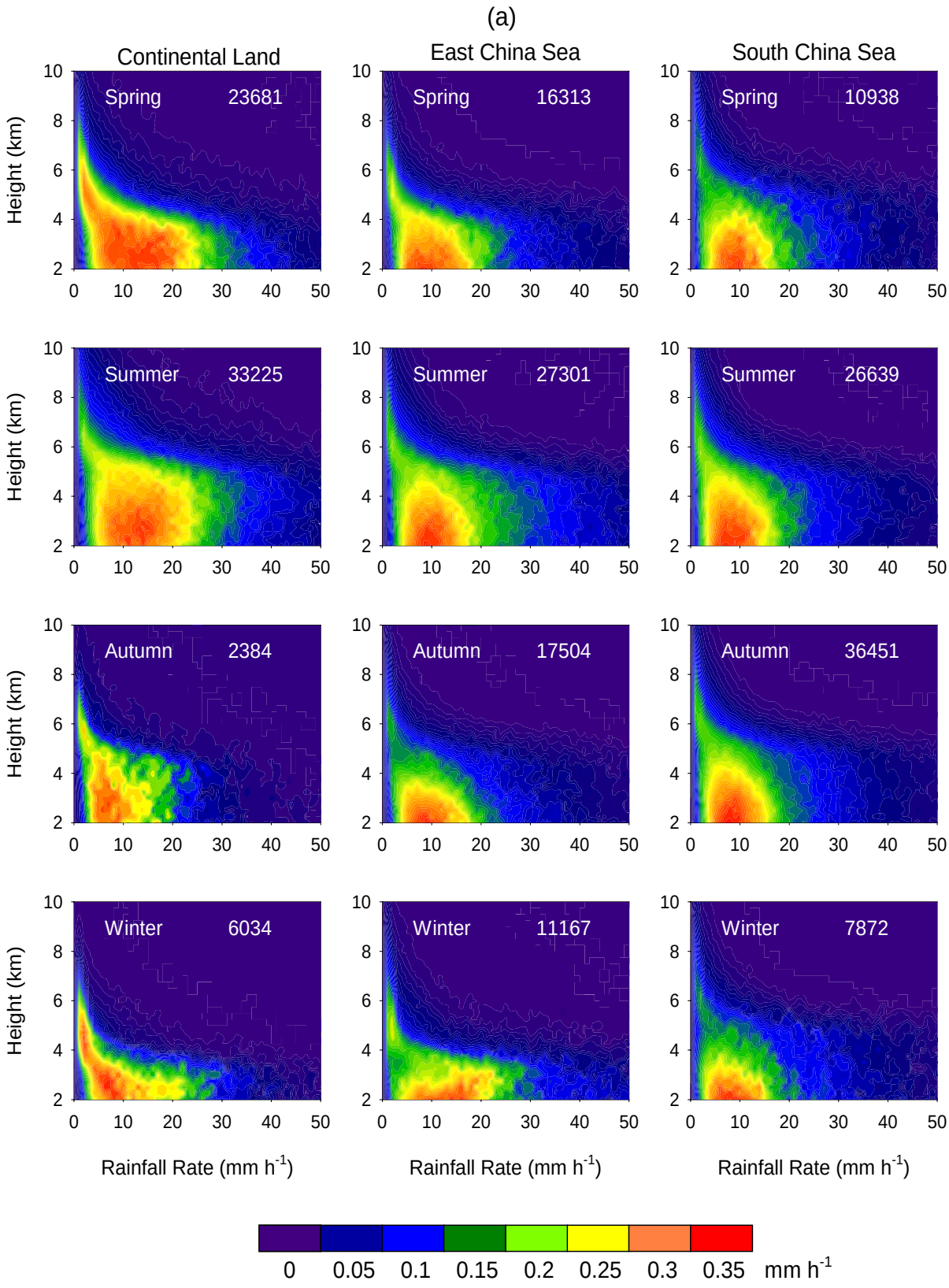

Fig. 5 CRADs of rainfall rates in the vertical for (a) deep convective and (b) stratiform rains from spring to winter. Number at the right top in each diagram is total numbers of profiles for a given rain type and season.

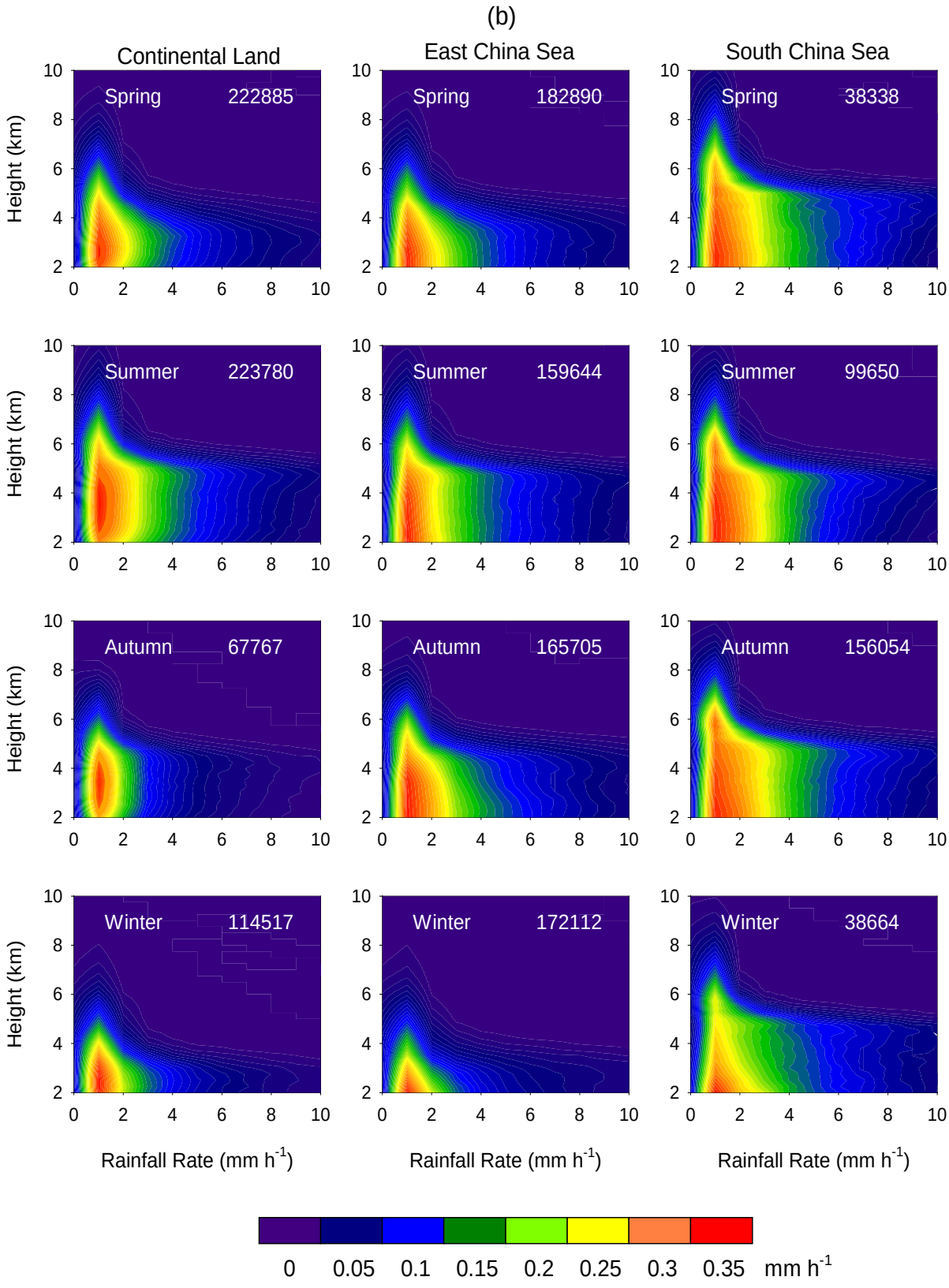

Fig. 5 (Continued)

It is noted in Figs. 5a and 5b that the maximum CRADs of deep convective rain occur near the surface over the ocean region, both the East China Sea and South China Sea. However, over the continental land the maximum appears at about 2.5 km altitude for deep convective rain at each season except in winter, and about 3 km for stratiform rain except in winter. This may be comprehended as an evaporation process occurring in the low altitude of precipitating cloud similar to tropical profiles (Liu and Fu, 2001) and discussed by Fujiyoshi et al. (1980), Hobbs (1989), and Liu and Takeda (1989). Another important point in Fig. 5a is that we can find a much greater ice component above the freezing level inside deep convective precipitating clouds over the continental land at each season.

In search for regularities of precipitation profiles, we used the method of principal component (PC) analysis in the tropics (Liu and Fu, 2001). Our results showed the first leading PC component can explain more than 80% of the variations in the profiles, and the reconstructed first principal components closely resemble the mean profiles. The mean profiles for deep convective and stratiform rains over the tropical ocean are shown in Fig. 6. Characteristics of the mean profiles were addressed (Liu and Fu, 2001). We find the same regulation for deep convective and stratiform rains in the three regions of East Asia (see Tables 2a and 2b). The predominance of the first PC implies that the mean profile is statistically meaningful enough to represent the characteristic pattern of vertical precipitation profiles. In other words, given a rain type (convective/stratiform) and a surface rainfall rate, the rainfall rate profile tends to follow the mean profile with statistically significant likelihood. This finding is interesting in the following two ways. First, it implies that there is a common physical process at work in the East Asia cloud systems that determines the general pattern of the rain vertical profiles. Second, it provides a constraint, at least in a statistical sense, to formulating models of vertical hydrometeor structures that can be used in satellite rain retrieval algorithms, or even to guiding the parameterization of rain processes in numerical models.

Based on the principal component analysis above, characteristics of mean precipitation profiles in the seasons are presented according to rainfall type and surface rain rate. Figure 7 displays a seasonal variability of precipitation profiles for both deep convective rain of 10 mm h^{-1} and stratiform rain of 5 mm h^{-1} at 2 km altitude in the three regions. It shows obvious differences in profiles between the summer and winter

Table 2a. Contribution to total variance (in %) by the first leading PCs for deep convections

	Land				East China Sea				South China Sea			
R	N	PC1	PC2	PC3	N	PC1	PC2	PC3	N	PC1	PC2	PC3
5	2585	71.8	14.0	5.2	2516	78.6	10.5	3.5	2577	76.8	11.0	4.0
10	2245	75.3	11.4	4.8	1698	82.8	7.8	3.1	1748	83.4	7.4	2.7
15	1686	81.3	8.2	3.3	938	83.7	7.0	3.0	595	83.2	7.3	2.8
20	1116	82.5	7.3	3.3	484	86.2	5.3	2.9	517	85.7	5.6	2.7
25	667	82.9	7.1	3.0	263	88.5	4.1	2.4	314	87.0	5.5	2.2
30	423	82.5	6.3	3.3	182	86.8	5.6	2.4	180	87.5	4.2	2.9

R: Rainfall rate (mm h^{-1})
N: Number of profiles

Table 2b. Contribution to total variance (in %) by the first leading PCs for stratiform rains

	Land				East China Sea				South China Sea			
R	N	PC1	PC2	PC3	N	PC1	PC2	PC3	N	PC1	PC2	PC3
1	2972	76.9	8.1	3.3	2800	78.2	8.0	3.1	1207	80.0	6.7	3.1
5	7081	85.6	4.7	2.2	7084	86.2	4.8	2.0	4543	88.1	4.2	1.5
10	1193	85.7	5.5	2.1	1475	87.8	4.2	2.0	599	89.2	3.7	2.5

R: Rainfall rate (mm h^{-1})
N: Number of profiles

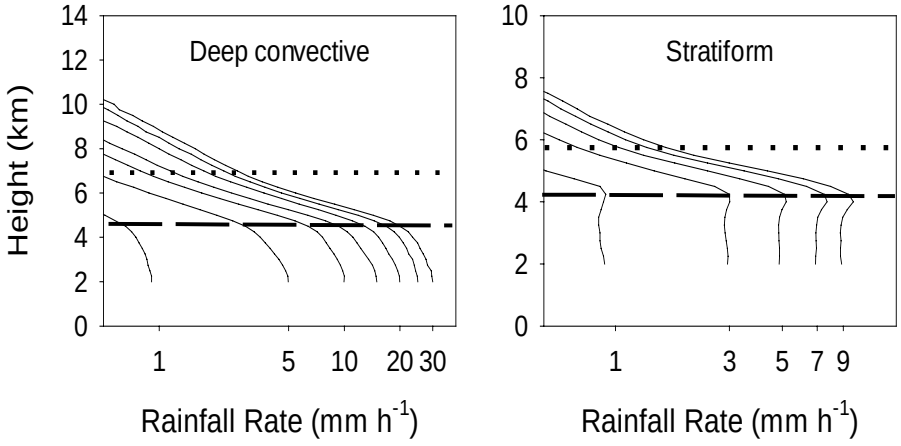

Fig. 6. Yearly mean profiles for deep convection (left panel) and stratiform (right panel) rains in the tropical ocean.

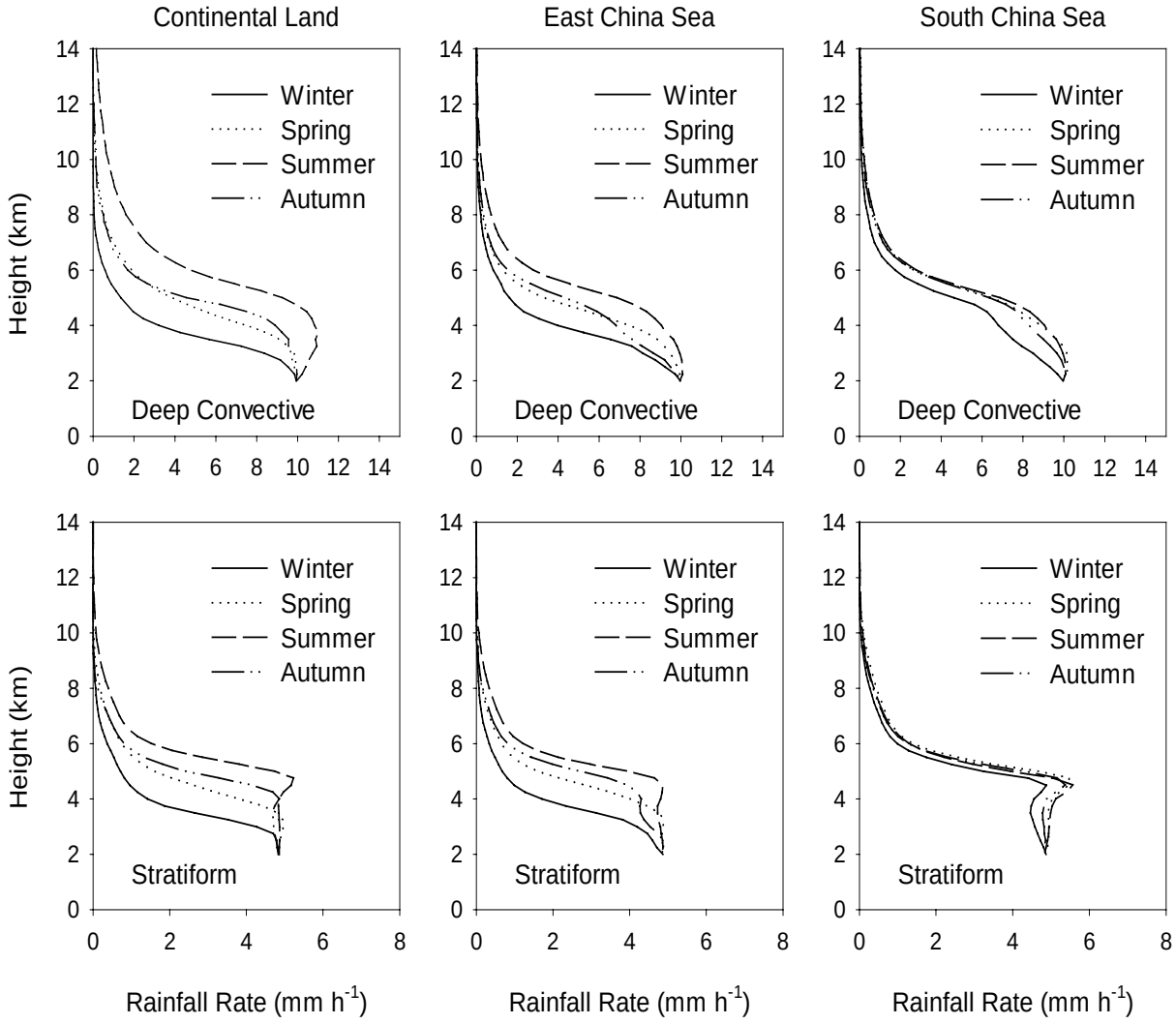

Fig. 7. Seasonal variations of mean profiles for deep convection (upper panel) and stratiform rains (blower panel) from spring to winter.

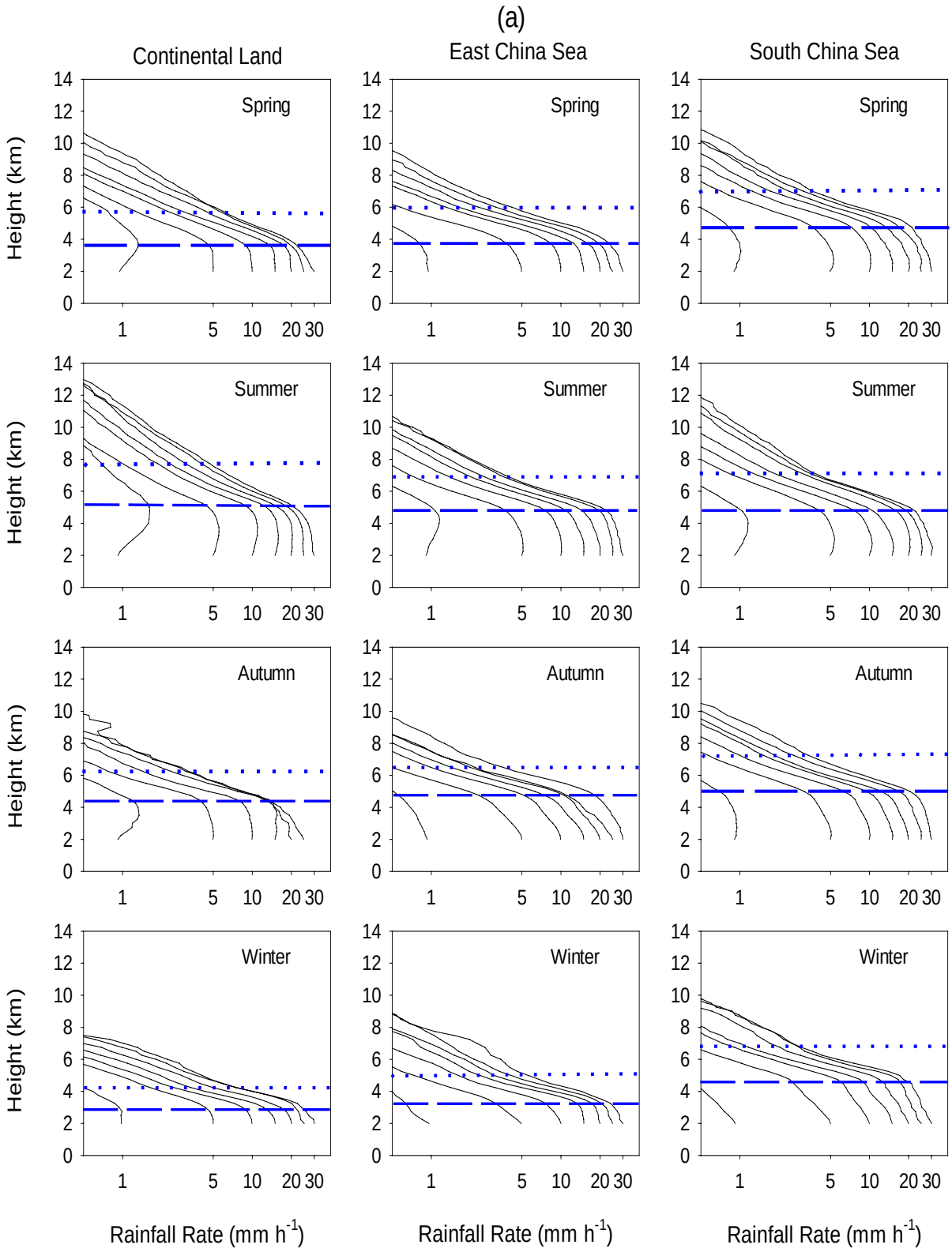

Fig. 8. Mean profiles from spring to winter in continental land, the East China Sea, and the South China Sea. (a) Deep convective profiles plotted at rainfall rates of 1, 5, 10, 15, 20, 25, and 30 mm h^{-1} at 2 km, (b) Stratiform profiles at rainfall rates of 1, 3, 5, 7, and 9 mm h^{-1} at 2 km.

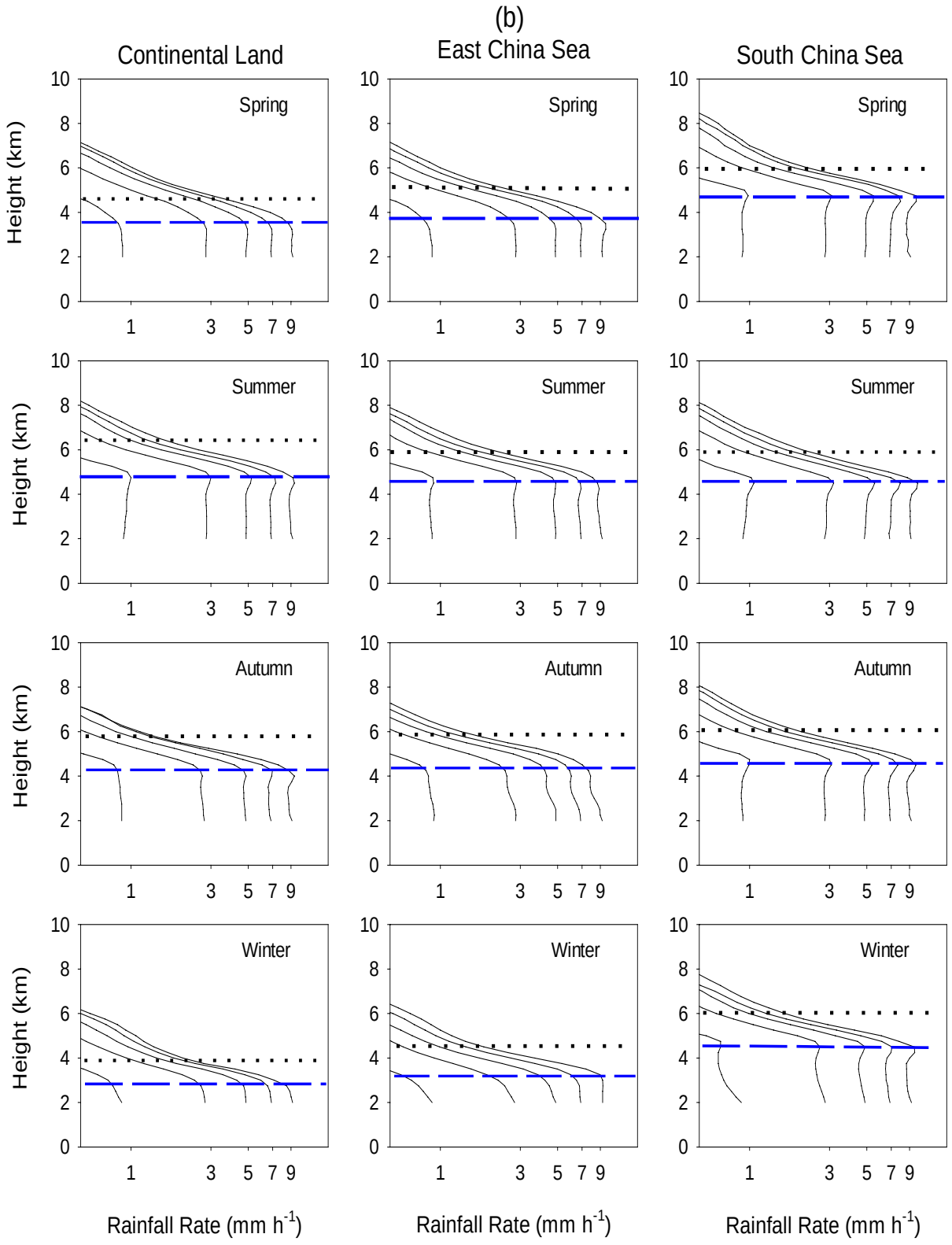

Fig. 8. (Continued)

in the mid-latitude region, especially in the continental land. The amplitude changes of profiles in spring and autumn are located between the summer and winter profiles. In the South China Sea, the differences are relatively small, except in winter. The feature is consistent with Figs. 5a and 5b. We conclude that the strongest seasonal variability of precipitation in vertical structures occurs over the continental land even though region of the East China Sea has the same latitude as the land. Such seasonal variability can be neglected over the South China Sea regardless of rain type (not including winter), i.e., the precipitations are basically of a tropical type in the region from spring to autumn.

For comprehensive seasonal characteristics, we present the mean profiles for deep convective and stratiform rains in each season in Figs. 8a and 8b, and the root mean square distributions in Figs. 9a and 9b. In these figures, deep convective profiles are plotted at rainfall rates of 1, 5, 10, 15, 20, 25, and 30 mm h^{-1}, and 1, 3, 5, 7, and 9 mm h^{-1} for stratiform. Due to limited samples, stratiform profiles for rain rates larger than 10 mm h^{-1} are not processed. For convenient comparison, we plot the mean rainfall rate on a logarithm scale.

Similar to the drawings in Figs. 5a and 5b, obvious, different profile patterns between deep convective and stratiform rains also appear in Figs. 8a and 8b regardless of which region. In the South China Sea, the features of mean stratiform profiles are the same as those discussed for the tropical ocean (Fig. 6) (but the difference between winter and the other seasons is not clear in Fig. 8b), i.e., the bright band near 4.5 km separates generally two totally different variation regimes. Below the bright band, the rain rates are almost constant in this layer (liquid water layer, or rain layer). In this layer, rainfall rates slightly decrease or increase toward the surface, implying that raindrops experience further growth by coagulation or evaporation processes. Above the bright band, a sharp downward growth of rain rates occurs within a layer about 1.25 km in depth, and is followed by a slower growth above. The 1.25 km depth layer should be one with a mixture of ice and water (the mixture layer). Above the layer, the profile reflects ice information, i.e., an ice layer with the slowest microphysical growth mode (e.g., Houze, 1993, Chapter 6). The mean stratiform profiles in the mid-latitude region have similar features. The only difference is that the three layers shift with the seasonal changes of the freezing level, and a little bit of thickening of the mixture layer occurs in spring and winter, especially over the continental land.

The mean profiles for deep convections in the South China Sea also display the same characteristics from spring to autumn as in the tropical ocean as discussed in our previous paper (Liu and Fu, 2001). There are two rain layers below the freezing level. One layer, the coagulation layer, is from the height of the stratiform bright band to the maximum of the rain rate (about 2.5 km altitude); the other very thin layer, the evaporation layer, is below the maximum rainfall rate. In winter, only the coagulation layer exists below the freezing level. Above the freezing level, the mixture layer and ice layer are clear in each season as they appear in the stratiform profiles. But the mixture layer of deep convective rain (about 1.5 km) is deeper than that of stratiform rain. Of course, the profile slopes above the freezing level between the deep convective and stratiform profiles are different, which should mark different microphysical processes in both precipitating clouds. We will address these features and their impacts on microwave brightness temperatures in the future.

In the East China Sea, the evaporation layer near the surface does not exist except in summer. The layer divisions (the rain layer, the mixture layer, and ice layer) are close to those in the South China Sea in winter, and their altitude varies with the seasons. In summer, the evaporation layer is clear near the surface. The situation is complex in the continental land, and profiles show the strongest seasonal variability. In summer, the layer divisions in the region are close to those in the South China Sea in the same season, i.e. deep convective rains over the continental land are of a tropical type in summer. However, we must note a deeper evaporation layer over the continental land due to strong activities of convective rains. In spring and autumn, the evaporation layer seems unclear, which is different from the CRADs figure. That may be the weakness of comparing mean profiles with CRADs. In winter, the three layers (ice layer, mixture layer, and rain layer) are depressed toward the surface due to the decrease in air temperatures.

Finally, we plot profile deviations from the mean profiles with root mean square (RMS) errors in Figs. 9a and 9b. One striking feature is the maximum value of RMSs appearing at the freezing level regardless of rain type,location,and season. The RMSs become larger when the surface rainfall rates increase. The maximum error is about 5–8 mm h^{-1} for a 10 mm h^{-1} surface rainfall rate, and 8–12 mm h^{-1} for 20 mm h^{-1}. The above implies a very complicated rain formation processes within the freezing level. In the near future, we will discuss the effects of these errors on microwave brightness temperatures when using mean profiles in a radiation transfer model.

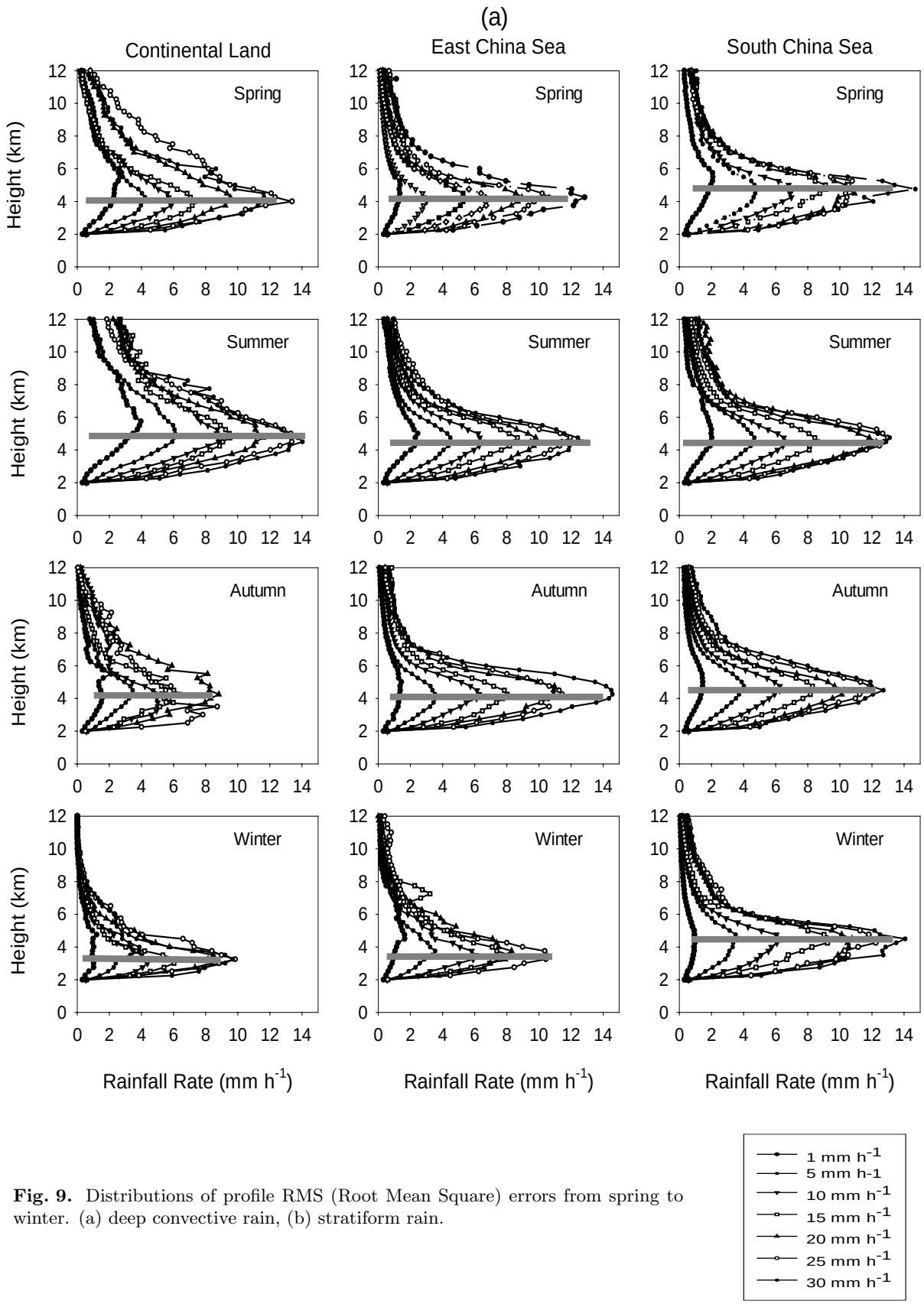

Fig. 9. Distributions of profile RMS (Root Mean Square) errors from spring to winter. (a) deep convective rain, (b) stratiform rain.

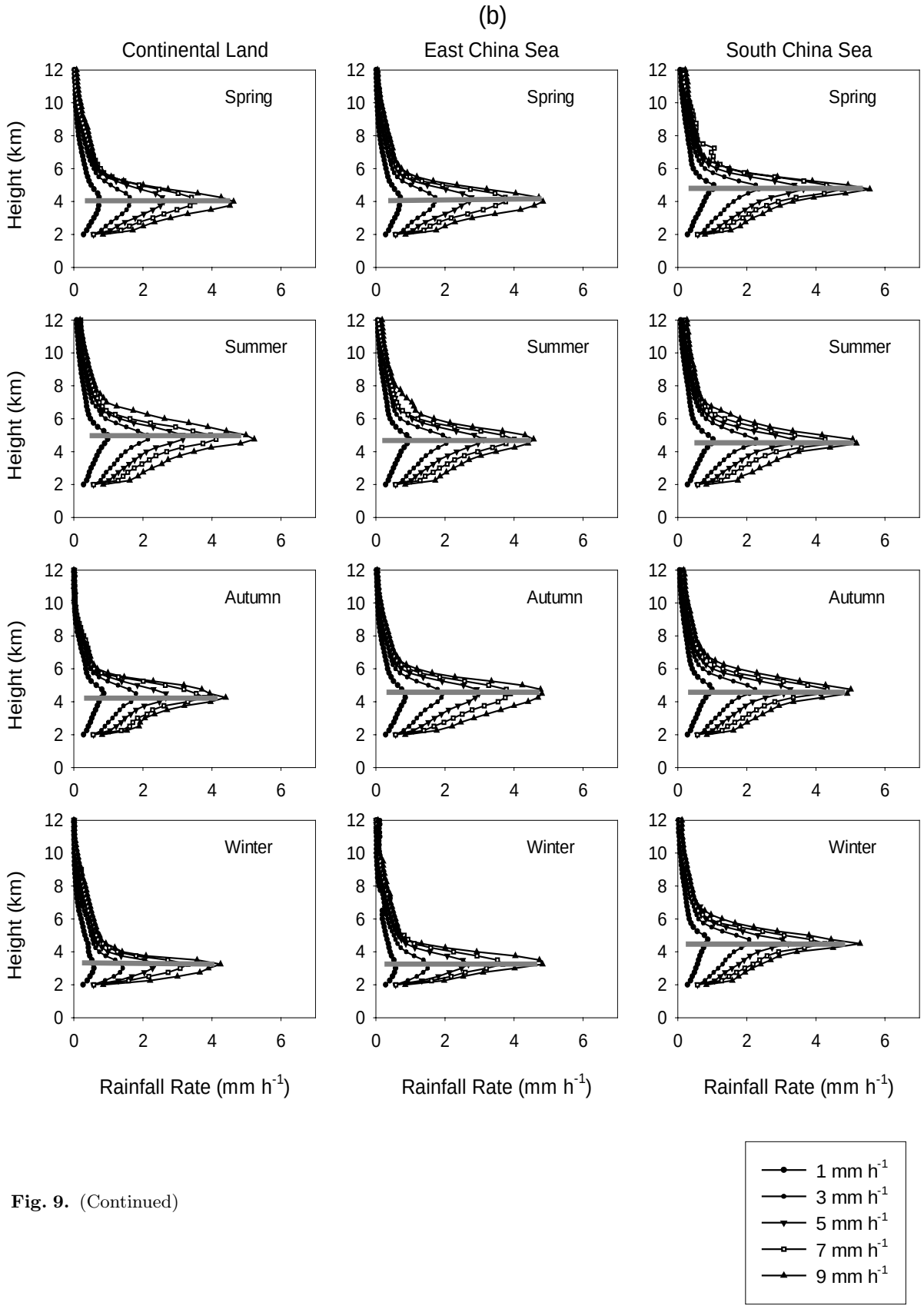

Fig. 9. (Continued)

4. Conclusions

In this study, we analyzed the seasonal characteristics of precipitations in East Asia with data observed by TRMM PR in 1998. We intended to regularize the horizontal distributions of precipitation events in East Asia on a seasonal scale, and the vertical structures of precipitation in the region.

Following the classification of precipitations in the standard TRMM product, 2A25, firstly, we studied sample statistics that shows about 83.7%, 13.6%, and 2.7% area fractions for stratiform, deep convective, and warm convective rains, respectively in East Asia, i.e. prevalent stratiform rains and unimportant warm rain events in East Asia. Deep convective rain has about one-sixth of the stratiform area fraction. However, it contributes nearly the same rainfall a mount to total rain (about 48%) as stratiform rain (about 50%). This is a little bit different from the tropics. In the tropics, the contributions to total rain by stratiform rain and deep convective rain are almost equally important, i.e., about 45% by stratiform and 42% by deep convective rain while the area fraction ratio of stratiform to deep convective rain is about 7. Studies indicate that the ratio of surface rainfalls produced by stratiform and deep convective rains are proportional to numbers of both rain types on a seasonal scale.

Before exposing horizontal distributions of deep convective and stratiform rains, we compared seasonal rainfall and its distribution generated by TRMM PR with GPCP output. Generally, the rainfall patterns are very close to each other in winter, spring, and autumn. In summer, however, there exists a difference in rainfall pattern and amplitude between the two datasets. It seems that the magnitude of surface rainfall estimated by GPCP is larger than that by TRMM PR detections. We are not sure which one is more accurate. Horizontal distributions of area fraction and rain fraction reveal that much more stratiform rain events and rainfall are located in the northern part of East Asia, in contrast to the high frequency and rainfall amount of deep convective rains in the southern part. Seasonal variations of precipitation are very significant in a northward shift of deep convective rain events and rainfall amount from winter to spring, and southward movement from summer to autumn. Such movement is opposite for stratiform rains. In this meaning, the activity of deep convective rains may be regarded as a good index for the summer monsoon, and stratiform rain for the winter monsoon, in the mid-latitudes of East Asia.

The vertical structures of precipitations in CRADs and averaged profiles illustrate significant differences between deep convective and stratiform rains, regardless of location and season. The seasonal variability of the structures is very remarkable in the mid-latitudes of East Asia. However, we can neglect such variability over the South China Sea regardless of rain type except in winter, i.e. the precipitations are basically of tropical type in the region from spring to autumn. Distributions of CRADs illustrate a wide range of surface rainfall rate for most deep convective rains, and light rainrate for most stratiform rains in East Asia, regardless of over land or ocean. They also show a wider range of surface rain rate for deep convective rains over the continental land than over the oceanic regions. For stratiform rains, their surface rainfall rates are wider in the South China Sea than in the mid-latitude region. The mean profile analysis of deep convective rains indicates that the vertical structure of precipitation over the South China Sea can be divided into 4 layers, ice layer, mixture layer, rain layer, and evaporation layer from the top to near the surface except in winter. The division is similar to that in our previous studies for precipitation in tropics. We can find the four layers in the mid-latitude, land, and ocean areas in summer. In the other seasons, the evaporation layer is not obvious. For stratiform rain, only three layers, ice layer, mixture layer, and rain layer, exist regardless of season and place. We also noticed that the mixture layer of deep convective rain is deeper than stratiform's. We determined the maximum value of RMSs appearing at the freezing level for both rain types in East Asia in each season. The RMSs increase with surface rainfall rate. This implies very complicated rain formation processes within the freezing level.

Acknowledgments. Helpful comments from Lü Daren and Wu Guoxiong at the Institute of Atmospheric Physics, CAS, are greatly appreciated. Comments from the anonymous reviewers were very helpful. Satellite radar data were provided by NASDA/EORC, Japan and NASA Goddard Space Flight Center, USA, through the TRMM project. This research was supported by the National Natural Science Foundation of China (40175015 and 40233031), the Chinese Academy of Sciences (KZCX2-208, ZKCX-SW-210), the Ministry of Science and Technology (2001CCA02200), EORC/NASDA of Japan (Proposal ID: 206), and the Outstanding Foundation of the University of Science and Technology of China (KJ0750).

REFERENCES

Adler, R. F., H. Y. M. Yeh, N. Prasad, W. K. Tao, and J. Simpson, 1991: Microwave simulations of a tropical rainfall system with a three-dimension cloud model. *J. Appl. Meteor.*, **30**, 924–953.

Awaka. J., T. Iguchi, and K. Okamoto, 1998: Early results on rain type classification by the Tropical Rainfall Measuring Mission (TRMM) precipitation radar.

Pro. 8th URSI commission F Open Symp., Averior, Portugal, 134–146.

Chen, L. X., M. Dong, and Y. N. Shao, 1992: The Characteristics of interannual variations on the East Asian monsoon. *J. Meteor. Soc. Japan*, **70**, 617–637.

Ding, Y. H., and E. R. Reiter, 1982: A relationship between planetary-waves persistent rains and thunderstorms in China. *Arch. Meteor. Geophys. Bioclim., Series B,*, **31**, 221–252.

Ding, Y. H., Y. Zhang, Q. Ma, and G. Q. Hu, 2001: Analysis of the large scale circulation features and synoptic systems in East Asia during the intensive observation period of GAME/HUBEX. *J. Meteor. Soc. Japan*, **79**, 277–300.

Fu Yunfei, and Huang Ronghui, 1997: Impacts of westerly anomalies over East Asia on westerly bursts over the western tropical and the occurrence of ENSO events. *Chinese Journal of Atmospheric Sciences*, **21**, 195–204.

Fu, Y., and G. Liu, 2001: The variability of tropical precipitation profiles and its impact on microwave brightness temperatures as inferred from TRMM data. *J. Appl. Meteor.*, **40**, 2130–2143

Fujiyoshi, Y., T. Takasugi, Y. Gocho, and T. Takeda, 1980: Radar-echo structure of middle-level precipitating clouds and the change of raindrops-Processes of mixing of precipitation particles falling from generating cells. *J. Meteor. Soc. Japan*, **58**, 203–216.

Fulton, R., and G. M. Heymsfield, 1991: Microphysical and radiative characteristics of convective clouds during COHMEX. *J. Appl. Meteor.*, **30**, 98–116.

Hobbs, P. V., 1989: Research on clouds and precipitation-past, present, and future. *Bull. Amer. Meteor. Soc.*, **70**, 282–285.

Houze, R. A., Jr., 1981: Structures of atmospheric precipitation systems–A global survey. *Radio Sci.*, **16**, 671–689.

Houze, R. A., Jr., 1993: Cloud Dynamics. Academic Press, Inc., New York, 573pp.

Huffman, G. J., R. F. Adler, B. Rudoff. U. Schneider, and P. R. Keehn, 1995: Global precipitation estimates based on a technique for combining satellite-based estimates, rain gauge analysis, and NWP model precipitation information. *J. Climate*, **8**, 1284–1295.

Krishnamuti, T. N., and H. N. Bhalme, 1976: Oscillations of a monsoon system. Part I. Observational aspects. *J. Atmos. Sci.*, **33**, 1937–1954.

Kummerow, C., and L. Giglio, 1994: A passive microwave technique for estimating rainfall and vertical structure information from space. Part I: Algorithm description. *J. Appl. Meteor.*, **33**, 3–18.

Kuo, Y.-H., and G. T.-J. Chen, 1990: The Taiwan area Mesoscale Experiment (TAMEX): An overview. *Bull. Amer. Meteor. Soc.*, **71**, 488–503.

Lau, K.-M., and M.-T. Li, 1984: The monsoon of East Asia and its global associations-A survey. *Bull. Amer. Meteor. Soc.*, **65**, 114–125.

Lau, K.-M., G. J. Yang, and S. Shen, 1988: Seasonal and intraseasonal climatology of summer monsoon rainfall over East Asia. *Mon. Wea. Rev.*, **116**, 18–37.

Liu, G., and T. Takeda, 1989: Two types of stratiform precipitating clouds associated with cyclones. *Tenki*, **36**, 147–157. (in Japanese)

Liu, G., and Y. Fu, 2001: The characteristics of tropical precipitation profiles as inferred from satellite radar measurements. *J. Meteor. Soc. Japan*, **79**, 131–143.

Matsumoto, J., 1985: Precipitation distribution and frontal zone over East Asia in summer of 1979. Bull. Dept. Geography, Univ. Tokyo No.17, 45–61.

Murakami, M., 1983: Analysis of deep convective activity over the western Pacific and Southeast Asia. *J. Meteor. Soc. Japan*, **61**, 60–75.

Ninomiya, K., 1984, Characteristics of the Baiu front as a predominant subtropical front in the summer Northern Hemisphere. *J. Meteor. Soc. Japan*, **62**, 880–894.

Ninomiya, K., 2000, Large- and meso-α-scale characteristics of the Meiyu/Baiu front associated with intense rainfalls in 1-10 July 1991. *J. Meteor. Soc. Japan*, **78**, 141–157.

Ninomiya, K., and T. Murakami, 1987: The early summer rainy season (Baui) over Japan. *Monsoon Meteorology*, P.-C. Chang and T. N. Krishnamurti, Eds., Oxford Univ. Press, 93–121.

Petty, G. W., 1994: Physical retrievals of over-ocean rain rate from multichannel microwave imagery. Part II: Algorithm implementation. *Meteor. Atmos. Phys.*, **54**, 101–121.

Smith, E. A., and A. Mugnai, 1988: Radiative transfer to space through a precipitating cloud at multiple microwave frequencies, Part II: Result and analysis. *J. Appl. Meteor.*, **27**, 1074–1091.

Szoke, E. J., E. J. Zipser, and D. P. Jorgensen, 1986: A radar study of convective cells in mesoscale systems in GATE. Part I: Vertical profile statistics and comparison with hurricanes. *J. Atmos. Sci.*, **43**, 182–197.

Takeda, T., and H. Iwaski, 1987: Some characteristics of meso-scale cloud clusters observed in East Asia between March and October 1980. *J. Meteor. Soc. Japan*, **60**, 507–513.

Tao, S. Y., and L. X. Chen, 1987: *Review in Monsoon Meteorology*, Oxford Univ. Press, 60–92.

Tao, W. -K., J. Simpson and R. F. Adler, 1993: Retrieval algorithms for estimating the vertical profiles of latent heat release: Their applications for TRMM. *J. Meteor. Soc. Japan*, **71**, 685–700.

Wilheit, T. T., A. T. C. Chang, M. S. V. Rao, E. B. Rodgers, and J. S. Theon, 1977: A satellite technique for quantitatively mapping rainfall rates over the oceans. *J. Appl. Meteor.*, **16**, 551–560.

Yasunari, T., 1990: Impact of Indian monsoon on the coupled atmosphere/ocean system in the tropical Pacific. *Meteor. Atmos. Phys.*, **44**, 29–41.

Yasunari, T, 1991, The monsoon year A new concept of the climate year in the tropics. *Bull. Amer. Meteor. Soc.*, **72**, 1331–1338.

Yuter, S. E., and R. A. Houze Jr., 1995: Three-dimensional kinematic and microphysical evolution of Florida cumulonimbus, Part III: Vertical mass transport, mass divergence, and synthesis. *Mon. Wea. Rev.*, **123**, 1964–1983.

Zipser, E. J., and K. R. Lutz, 1994: The vertical profile of radar reflectivity of convective cells: A strong indicator of storm intensity and lightning probability? *Mon. Wea. Rev.*, **122**, 1751–1759.

TRMM 测雨雷达对1998年东亚降水季节性特征的研究

傅云飞　林一骅　刘国胜　王 强

摘　　要

利用热带测雨计划卫星上的测雨雷达得到的降水资料，对1998年东亚降水，特别是中国大陆东部、东海和南海的降水，进行了分析研究，并对比了热带降水研究结果。年统计结果表明，东亚地区层状云降水出现概率极高(比面积达83.7%)，对流云降水的比面积仅占13.6%，然而两者对总降水量的贡献相当。结果还表明，暖对流云降水出现的比例和对总降水量的贡献很小。在季节尺度，对流云和层状云降水的比与两者的面积比成比例关系。除夏季外，测雨雷达降水量与GPCP降水量可比性好。研究结果还指出：在中纬度陆地和海洋上对流云和层状云的比降水量和比面积呈相反方向作季节性南北移动，这一活动与东亚季风变化一致；该地区降水的季节性变化还表现为降水垂直廓线的变化。除冬季外，南海地区降水垂直结构呈热带特征。CRAD分析表明，对流云降水的地面雨强变化大，尤其在陆地上，而层状云多表现为地面弱降水。

关键词: TRMM测雨雷达，季节变化，降水结构